Recent advances in reduced-order modeling for transport phenomena

NETL 2009 Workshop on
Multiphase Flow Science
Morgantown, WV, April 22-23, 2009

Tom Brenner
Raymond Fontenot
Paul Cizmas

Texas A&M University

Outline

- Introduction
  - Track B 4 - reduced-order models from accurate computational results for use by design engineers
- Proper orthogonal decomposition (POD)
  - POD basics
  - Acceleration and error reduction
- POD for moving discontinuities
  - Discontinuity (bubble) detection
  - Augmented POD
- Three-dimensional POD implementation
- Conclusions and future work

Introduction

- Governing equations for transport phenomena are highly non-linear PDEs and therefore CPU intensive
- Need fast approximate solution for design purposes that allows a wide range of cases to be simulated quickly
- Reduced-order models based on proper orthogonal decomposition (POD) are optimal choice
- Goal is to develop accurate and efficient POD methods and implement them for MFIX

Proper Orthogonal Decomposition

Proper Orthogonal Decomposition (POD) Method

- POD is also known as Singular Value Decomposition, Karhunen-Loeve Decomposition, Principal Components Analysis, and Singular Systems Analysis
- Provides optimal basis for modal decomposition of a data set
- Extracts key **spatial** features from physical systems with spatial and temporal characteristics
- Reduces a large set of governing PDEs to a much smaller set of ODEs

POD Method

- Extracts:
  - time-independent orthonormal basis functions $\Phi_k(x)$
  - time-dependent orthonormal amplitude coefficients $\alpha_k(t_i)$ such that the reconstruction

$$u(\mathbf{x}, t_i) = \sum_{k=1}^{M} \alpha_k(t_i)\varphi_k(\mathbf{x}), \qquad i = 1, \ldots, M$$

is optimal in the sense that the average least square truncation error

$$\varepsilon_m = \left\langle \left\| u(\mathbf{x}, t_i) - \sum_{k=1}^{m} \alpha_k(t_i)\, \varphi_k(\mathbf{x}) \right\|^2 \right\rangle \qquad (1)$$

is a minimum for any given number $m \leq M$ of basis functions over all possible sets of orthogonal functions

POD Method

- Optimal property (1) reduces to:

$$\int_D \langle u(\mathbf{x})u^*(\mathbf{y})\rangle \varphi(\mathbf{y})dy = \lambda\varphi(\mathbf{x}) \qquad (2)$$

$\{\Phi_k\}$ are eigenfunctions of integral equation (2), whose kernel is the averaged autocorrelation function

$$\langle u(\mathbf{x})u^*(\mathbf{y})\rangle \equiv R(\mathbf{x},\mathbf{y}) \qquad (3)$$

- For a finite-dimensional case, (3) replaced by tensor product matrix

$$\overline{\overline{R}}(\mathbf{x},\mathbf{y}) = \frac{\sum_{i=1}^{M} u(\mathbf{x},t_i)u^T(\mathbf{y},t_i)}{M}$$

Acceleration Methods

- Database splitting
- Algorithm for quasi-symmetric **A** matrix
- Freezing **A** matrix
- Initial time step adjustment used in combination with database splitting
- Variable snapshot distribution
- Coupled vs. split autocorrelation matrices

Model Problem

Table 1: Parameters of fluidized bed.

Parameter	Description	Units	
x_{length}	Length of the domain in x-direction	cm	25.4
y_{length}	Length of the domain in y-direction	cm	76.5
	Number of cells in x-direction	-	108
	Number of cells in y-direction	-	124
v_1, v_2	Gas inflow velocities	cm/s	12.6, 1
p_{g_s}	Static pressure at outlet	g/cm/s^2	$1.01e^6$
T_{g0}	Gas temperature	K	297
μ_{g0}	Gas viscosity	g/cm/s	$1.8e^{-4}$
t_{start}	Start time	s	0.2
t_{stop}	Stop time	s	1.0
ρ_s	Particle density	g/cm^3	1.0
D_p	Particle diameter	cm	0.05
h_{s0}	Initial height of packed bed	cm	38.25
ϵ_g^*	Initial void fraction of packed bed	-	0.4

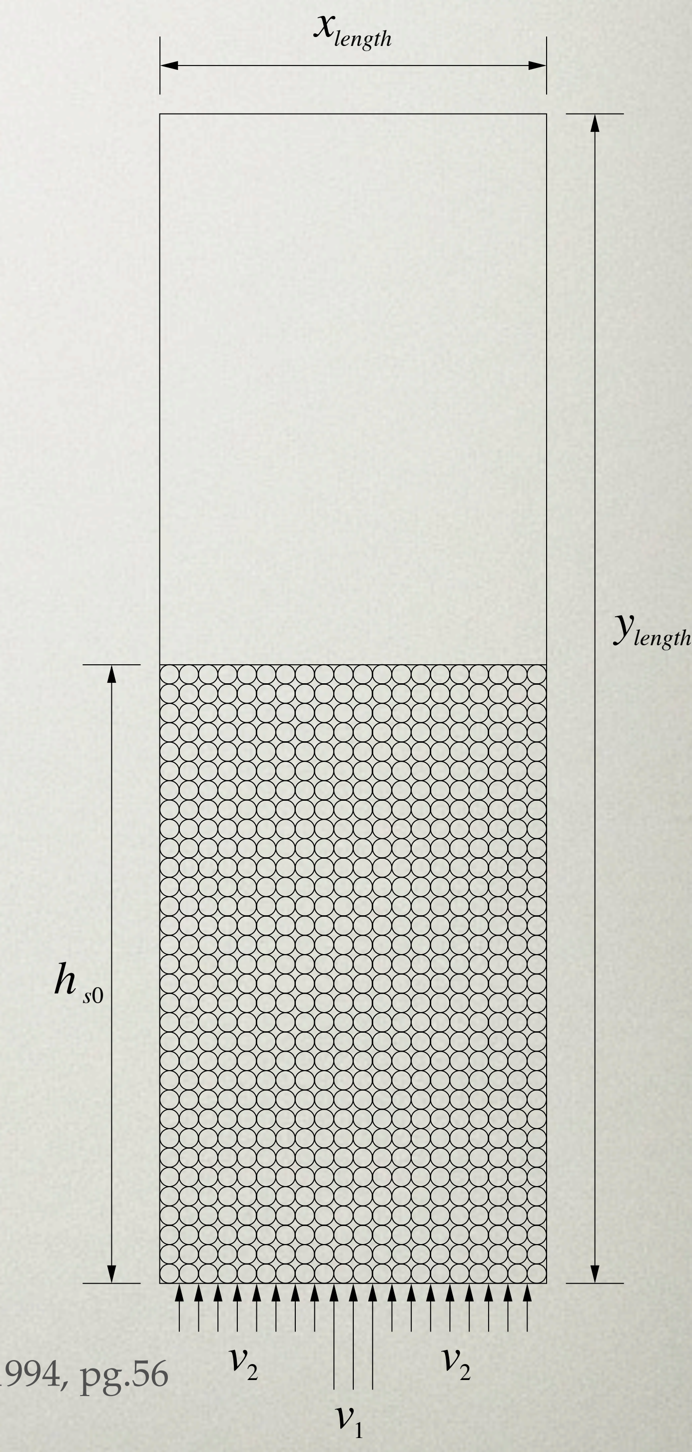

Gidaspow, *Multiphase Flow and Fluidization, Continuum and Kinetic Theory Descriptions*, 1994, pg.56

POD Modes

Field variable	Symbol	No. of modes
Gas pressure	N_{p_g}	2
Solids volume fraction	N_{ϵ_s}	7
u gas velocity	N_{u_g}	2
v gas velocity	N_{v_g}	5
u solids velocity	N_{u_s}	8
v solids velocity	N_{v_s}	6

$$\aleph(\mathbf{x}, t_i) = \sum_{k=0}^{N_\aleph} \alpha_k^\aleph(t_i)\varphi_k^\aleph(\mathbf{x}), \qquad i = 1, \ldots, M$$

Acceleration Methods Results

	Speed-up Factor	Error, ε_{avg}
FOM	1	0
ROM with no acceleration	23	1.882E-2
ROM with database splitting	25	4.370E-2
ROM with projection freezing	24	0.151818
ROM with initial time step adjustment	52	9.879E-3
ROM with database splitting and initial time step adjustment	137	6.240E-2

Cizmas, Richardson, Brenner, O'Brien, and Breault, "Acceleration techniques for reduced-order models based on proper orthogonal decomposition," 2008

Error vs. Acceleration Method V_G

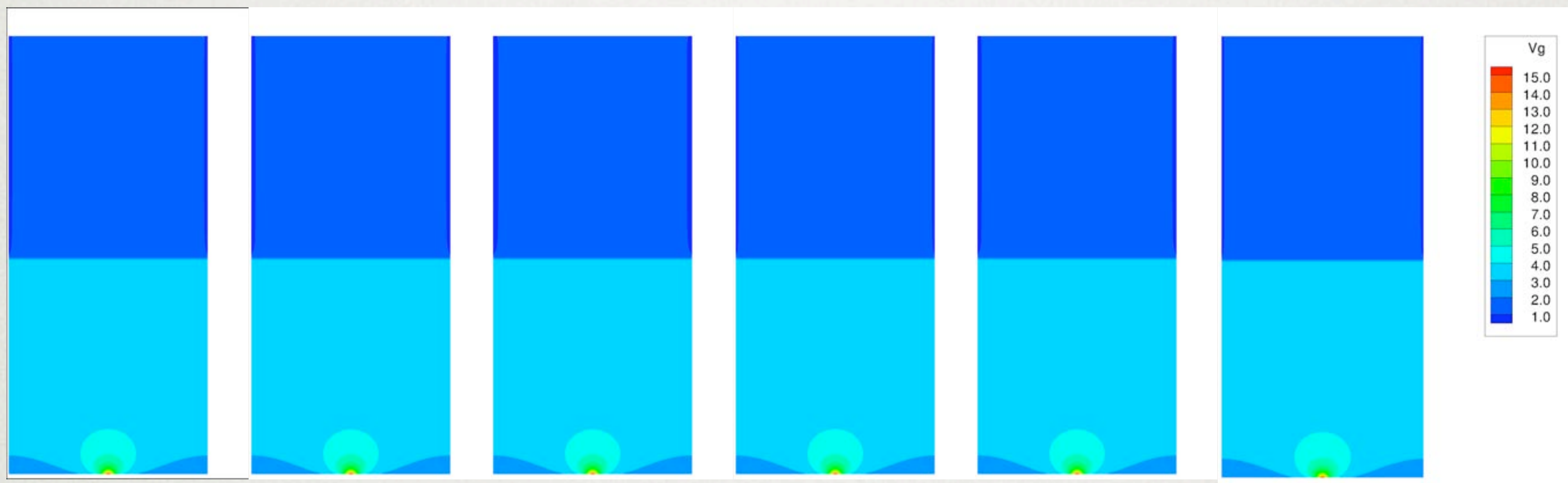

(a) (b) (c) (d) (e) (f)

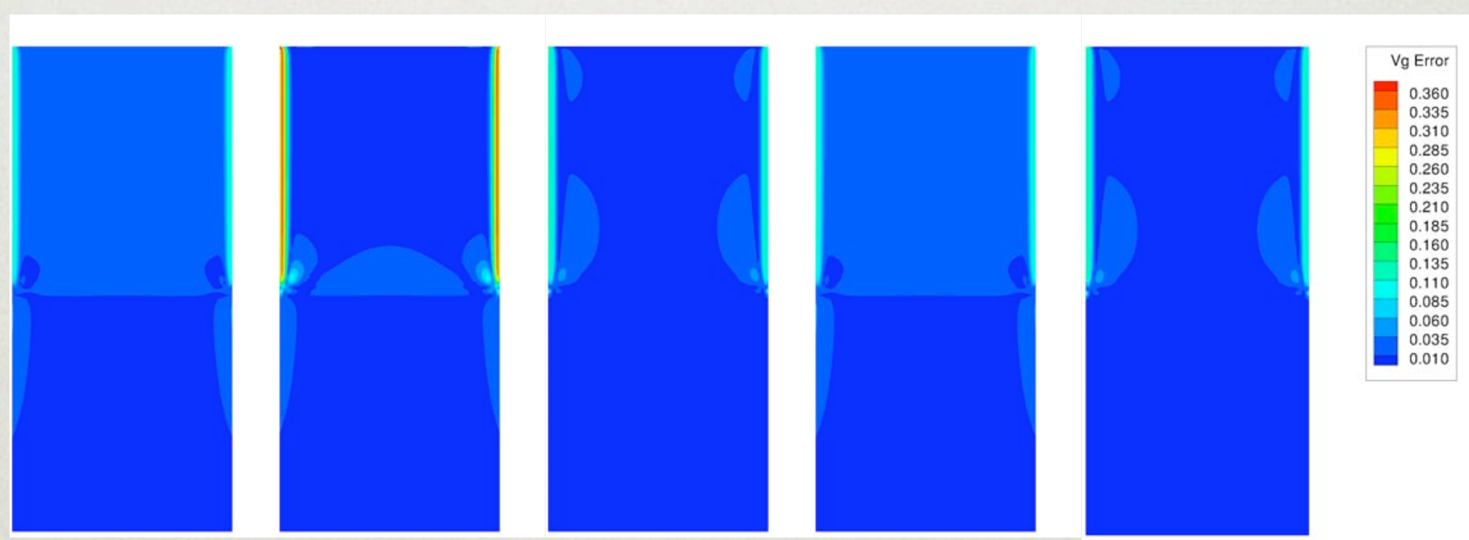

(g) (h) (i) (j) (k)

(a) FOM, (b) ROM, no acceleration, (c) ROM, matrix freezing, (d) ROM, database splitting, (e) ROM, initial time step adjustment, (f) ROM, database splitting and initial time step adjustment; and the gas velocity difference between (g) FOM and ROM, no acceleration, (h) FOM and ROM, matrix freezing, (i) FOM and ROM, database splitting, (j) FOM and ROM, initial time step adjustment, and (k) FOM and ROM, database splitting and initial time step adjustment (all values at t = 1.0 s).

Snapshot Sampling

Snapshot Distributions

- Constant sampling rate
  - Time between snapshots varied from 0.1 s to 0.001 s (8 to 800 snapshots)
- Constant sampling rate on subintervals (aka Step method)
  - Time domain divided into two subintervals
- Variable sampling rate
  - Time between snapshots based on a logarithmic curve fit

Computational vs. Physical Time

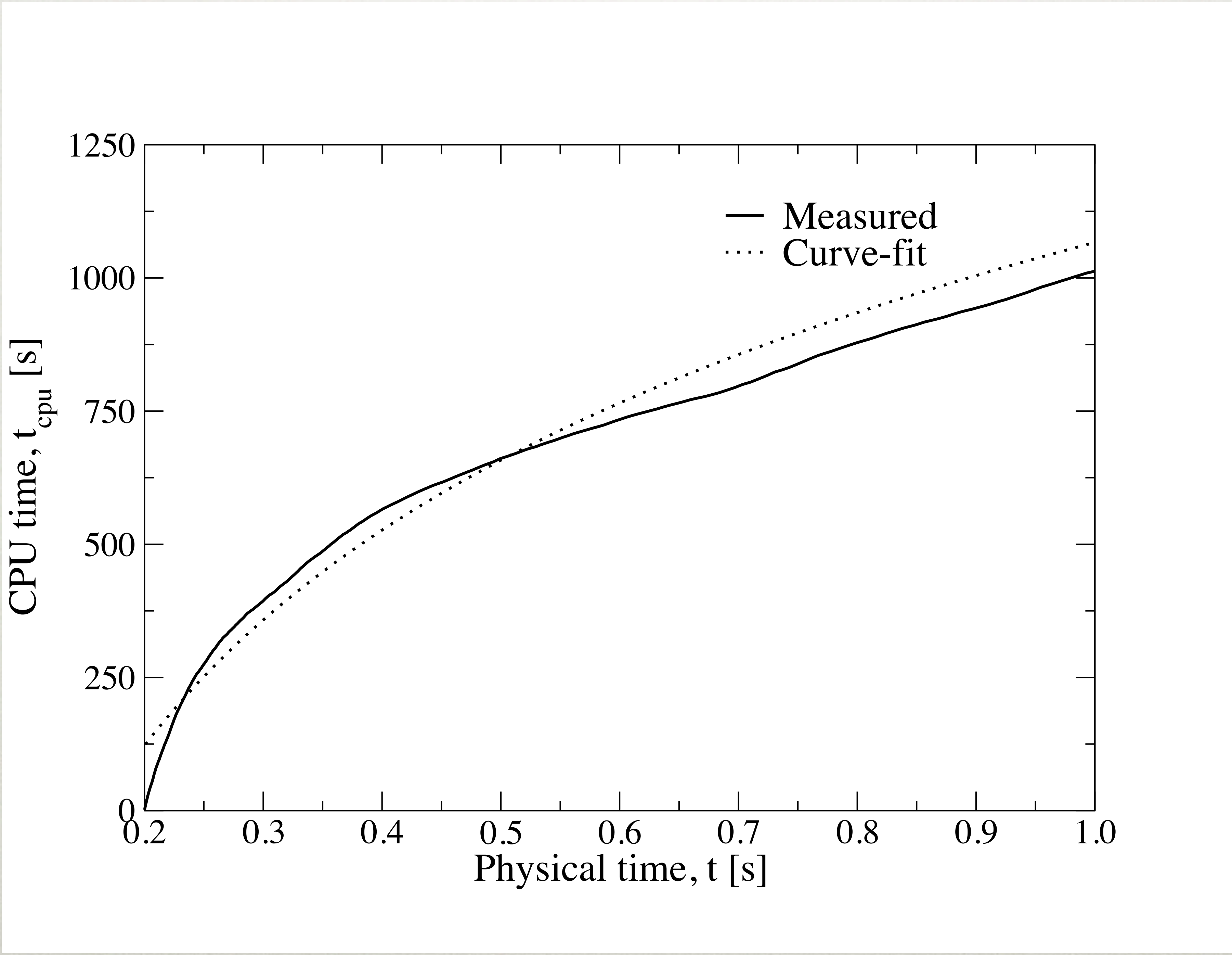

Continuously Varying Sampling Rate

Curve fit for computational time:

$$\mathrm{t}_{cpu}(t) = 588.14\ln(t) + 1071.0$$

Sampling time interval

$$dt(t_i) = \alpha\ln(t_i) + \beta$$

$$\frac{\alpha}{\beta} = \text{constant}$$

subject to

$$\sum_{i=1}^{M} dt(t_i) = t_M - t_1$$

so M and α / β uniquely determine

$$dt(t_i) = 0.00419\ln(t_i) + 0.00763$$

times for snapshot collection:

$$t_{i+1} = t_i + dt(t_i)$$

Step Method[‡]

- Decompose flow into two regions: transient and quasi-steady
- Transient region is from 0.2 s to 0.35 s
- Quasi-steady region is from 0.35 s to 1.0 s
- Collect 100 snapshots in each region, using a constant sampling rate
- Gives better snapshot resolution in the regions of greater flow complexity without the difficulties of devising a continuously varying distribution

‡ Park and Lee, "An Efficient Method of Solving the Navier-Stokes Equations for Flow Control," 1998

Sampling Methods

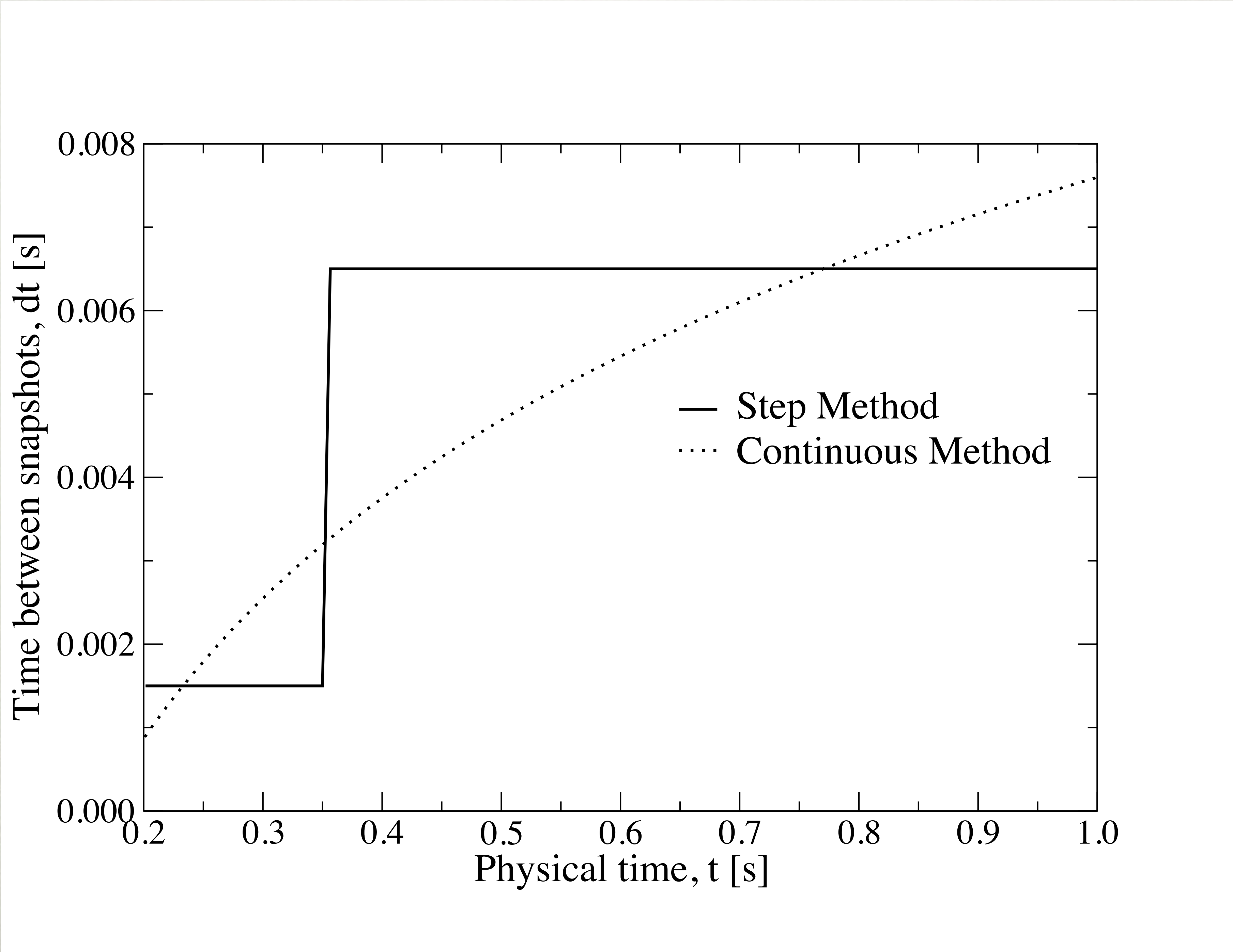

Results

Time between snapshots, dt, [s]	No. of snapshots	u_g	v_g	u_s	Error, ϵ v_s	ϵ_g	p_g
0.1	8	0.166	48.628	4.324E-003	0.584	5.737E-006	3.424E+006
0.075	12	0.167	30.761	5.840E-003	0.518	5.305E-006	1.977E+006
0.05	16	0.166	58.420	6.459E-003	0.558	3.204E-006	3.978E+006
0.025	32	0.163	21.339	6.328E-003	0.478	6.342E-006	1.240E+006
0.01	80	0.161	14.513	1.539E-003	0.195	4.507E-007	6.779E+005
0.0075	108	0.160	1.165	5.346E-004	1.149E-002	1.438E-008	3.883E+004
0.005	160	0.161	1.709	1.052E-003	1.401E-002	1.578E-008	9.977E+004
0.0025	320	0.160	0.812	3.675E-004	2.059E-003	2.014E-009	9.807E+003
0.001	800	0.160	0.247	1.315E-004	1.937E-004	1.781E-009	1.287E+003
0.004	200	0.161	0.981	1.533E-003	9.015E-003	4.617E-009	4.406E+004
0.0015 and 0.0065	202	0.165	0.261	1.968E-004	2.488E-004	1.911E-008	1.456E+003
varied from 9.2E-4 to 0.0075	197	0.165	0.241	1.439E-004	3.525E-004	3.372E-008	1.254E+003

$$\varepsilon = \left\langle \left\| u(\mathbf{x}, t_i) - \sum_{k=1}^{m} \alpha_k(t_i)\, \varphi_k(\mathbf{x}) \right\|^2 \right\rangle$$

Coupled vs. Split Autocorrelation Matrix

Coupled Approach

Scaled concatenated variable, $\tilde{u}$

$$\tilde{u}(\mathbf{x},t_i) = \begin{pmatrix} \tilde{u}_g(\mathbf{x},t_i) \\ \tilde{v}_g(\mathbf{x},t_i) \\ \tilde{u}_s(\mathbf{x},t_i) \\ \tilde{v}_s(\mathbf{x},t_i) \\ \tilde{\epsilon}_g(\mathbf{x},t_i) \\ \tilde{p}_g(\mathbf{x},t_i) \end{pmatrix} \qquad \tilde{\aleph} = \frac{\aleph}{\aleph_{max}}$$

$$\overline{\overline{R}}_c = \begin{pmatrix} \overline{\overline{R}}_{11} & \overline{\overline{R}}_{12} & \dots & \overline{\overline{R}}_{1N} \\ \overline{\overline{R}}_{21} & \overline{\overline{R}}_{22} & \dots & \overline{\overline{R}}_{2N} \\ \vdots & \vdots & \ddots & \vdots \\ \overline{\overline{R}}_{N1} & \overline{\overline{R}}_{N2} & \dots & \overline{\overline{R}}_{NN} \end{pmatrix}$$

N - spatial dimension

$$\overline{\overline{R}}_c \in \mathbb{R}^{6N} \times \mathbb{R}^{6N}$$

$$\overline{\overline{R}}_{ij} = \begin{pmatrix}
\langle \tilde{p}_{gi} * \tilde{p}_{gj} \rangle & \langle \tilde{\epsilon}_{gi} * \tilde{p}_{gj} \rangle & \langle \tilde{u}_{gi} * \tilde{p}_{gj} \rangle & \langle \tilde{v}_{gi} * \tilde{p}_{gj} \rangle & \langle \tilde{u}_{si} * \tilde{p}_{gj} \rangle & \langle \tilde{v}_{si} * \tilde{p}_{gj} \rangle \\
\langle \tilde{p}_{gi} * \tilde{\epsilon}_{gj} \rangle & \langle \tilde{\epsilon}_{gi} * \tilde{\epsilon}_{gj} \rangle & \langle \tilde{u}_{gi} * \tilde{\epsilon}_{gj} \rangle & \langle \tilde{v}_{gi} * \tilde{\epsilon}_{gj} \rangle & \langle \tilde{u}_{si} * \tilde{\epsilon}_{gj} \rangle & \langle \tilde{v}_{si} * \tilde{\epsilon}_{gj} \rangle \\
\langle \tilde{p}_{gi} * \tilde{u}_{gj} \rangle & \langle \tilde{\epsilon}_{gi} * \tilde{u}_{gj} \rangle & \langle \tilde{u}_{gi} * \tilde{u}_{gj} \rangle & \langle \tilde{v}_{gi} * \tilde{u}_{gj} \rangle & \langle \tilde{u}_{si} * \tilde{u}_{gj} \rangle & \langle \tilde{v}_{si} * \tilde{u}_{gj} \rangle \\
\langle \tilde{p}_{gi} * \tilde{v}_{gj} \rangle & \langle \tilde{\epsilon}_{gi} * \tilde{v}_{gj} \rangle & \langle \tilde{u}_{gi} * \tilde{v}_{gj} \rangle & \langle \tilde{v}_{gi} * \tilde{v}_{gj} \rangle & \langle \tilde{u}_{si} * \tilde{v}_{gj} \rangle & \langle \tilde{v}_{si} * \tilde{v}_{gj} \rangle \\
\langle \tilde{p}_{gi} * \tilde{u}_{sj} \rangle & \langle \tilde{\epsilon}_{gi} * \tilde{u}_{sj} \rangle & \langle \tilde{u}_{gi} * \tilde{u}_{sj} \rangle & \langle \tilde{v}_{gi} * \tilde{u}_{sj} \rangle & \langle \tilde{u}_{si} * \tilde{u}_{sj} \rangle & \langle \tilde{v}_{si} * \tilde{u}_{sj} \rangle \\
\langle \tilde{p}_{gi} * \tilde{v}_{sj} \rangle & \langle \tilde{\epsilon}_{gi} * \tilde{v}_{sj} \rangle & \langle \tilde{u}_{gi} * \tilde{v}_{sj} \rangle & \langle \tilde{v}_{gi} * \tilde{v}_{sj} \rangle & \langle \tilde{u}_{si} * \tilde{v}_{sj} \rangle & \langle \tilde{v}_{si} * \tilde{v}_{sj} \rangle
\end{pmatrix}$$

$$\overline{\overline{R}}_{ij} \in \mathbb{R}^6 \times \mathbb{R}^6$$

Split Approach

$$\overline{\overline{R}}_s = \begin{pmatrix} \overline{\overline{R}}_{\langle p_g * p_g \rangle} & 0 & 0 & 0 & 0 & 0 \\ 0 & \overline{\overline{R}}_{\langle \epsilon_g * \epsilon_g \rangle} & 0 & 0 & 0 & 0 \\ 0 & 0 & \overline{\overline{R}}_{\langle u_g * u_g \rangle} & 0 & 0 & 0 \\ 0 & 0 & 0 & \overline{\overline{R}}_{\langle v_g * v_g \rangle} & 0 & 0 \\ 0 & 0 & 0 & 0 & \overline{\overline{R}}_{\langle u_s * u_s \rangle} & 0 \\ 0 & 0 & 0 & 0 & 0 & \overline{\overline{R}}_{\langle v_s * v_s \rangle} \end{pmatrix}$$

$$\overline{\overline{R}}_s \in \mathbb{R}^{6N} \times \mathbb{R}^{6N}$$

$$\overline{\overline{R}}_{\langle \aleph * \aleph \rangle} = \frac{\sum_{i=1}^{M} \aleph(\mathbf{x}, t_i) \aleph^T(\mathbf{y}, t_i)}{M}$$

M - number of snapshots

Comparison of Results for Split and Coupled Approaches

Variable	Error			
	$\varepsilon^{coupled}$	ε^{split}	$\varepsilon_{rel}^{coupled}$	$\varepsilon_{rel}^{split}$
p_g	1.245E+006	57.91	1.230	5.72E-007
ϵ_g	1.012E-005	5.891E-010	1.012E-005	5.891E-010
u_g	1.305E-002	5.081E-003	9.758E-004	3.799E-004
v_g	1.380	8.980E-003	8.944E-002	5.820E-004
u_s	4.251E-005	4.833E-006	3.271E-004	3.719E-005
v_s	2.248E-004	4.866E-005	1.613E-003	3.491E-004

$$\varepsilon = \left\langle \left\| u(\mathbf{x}, t_i) - \sum_{k=1}^{m} \alpha_k(t_i)\, \varphi_k(\mathbf{x}) \right\|^2 \right\rangle$$

$$\varepsilon_{rel} = \frac{\varepsilon}{\aleph_{max}}$$

POD for Moving Discontinuities

Moving Discontinuities & POD

- Examples of moving discontinuities
  - Bubbles in multiphase flow
  - Shocks in transient high-speed gas flow
- Techniques
  - Domain decomposition
    - Nozzle flow†
    - Panel flutter‡

† Lucia, King, Beran, and Oxley, "Reduced Order Modeling for a One-Dimensional Nozzle Flow with Moving Shocks," AIAA-2001-2602

‡ Beran, Lucia, Pettit, "Reduced-order modelling of limit-cycle oscillation for aeroelastic systems," J. Fluids and Structures 19 (2004)

Bubbling Case: Geometry

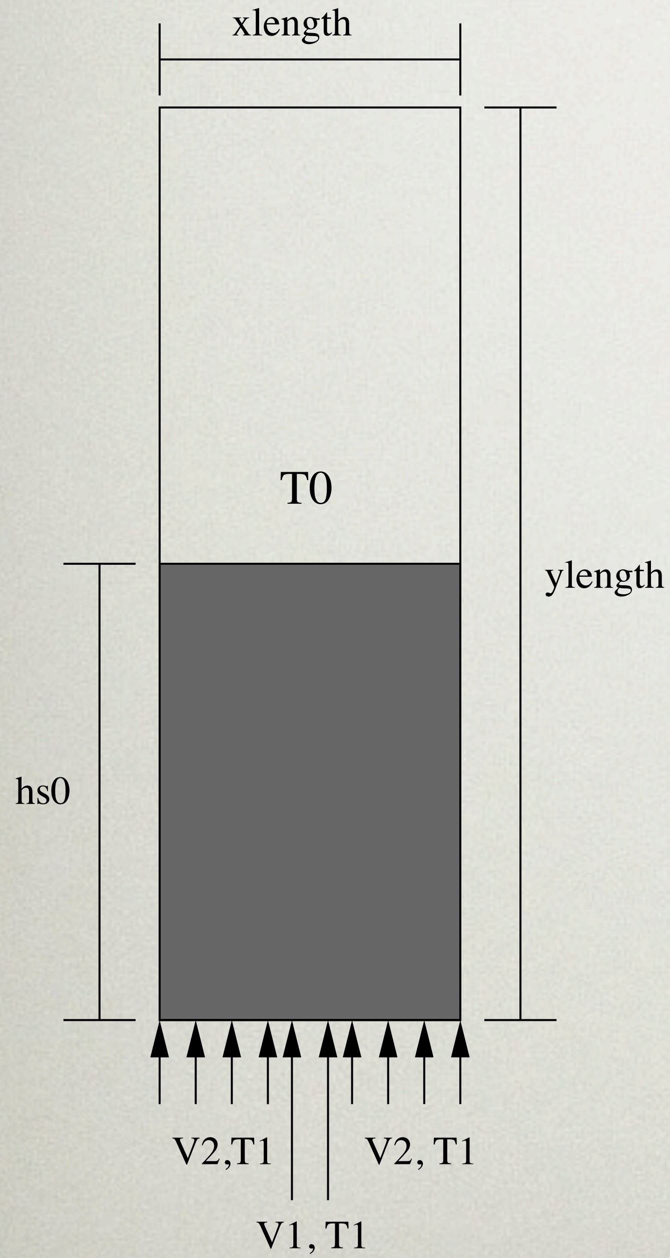

Parameter	Description	Value
x_{length}	Length of the domain in x-direction	40.0cm
y_{length}	Length of the domain in y-direction	76.5cm
$imax$	Number of cells in x-direction	108
$jmax$	Number of cells in y-direction	124
v_1	Jet gas inflow velocity	577.0cm/s
v_2	Distributed gas inflow velocity	53.6cm/s
p_s	Static gas pressure at outlet	1.01×10^6g/(cm$\cdot s^2$)
T_{g0}	Gas temperature	297K
μ_{g0}	Gas viscosity	1.8×10^{-4}g/(cm$\cdot$ s)
t_{start}	Start time	0s
t_{stop}	Stop time	5s
$\triangle t$	Initial time step	1.0×10^{-4}s
ρ_{so}	Constant solids density	2.42g/cm^3
D_p	Solids particle diameter	0.8mm
h_{s0}	Initial packed bed height	29.2cm
ϵ_g^*	Packed bed void fraction	0.40

Gidaspow, “Multiphase Flow and Fluidization,” pg. 158

Void Fraction:
T = 1.0 - 2.0 sec.

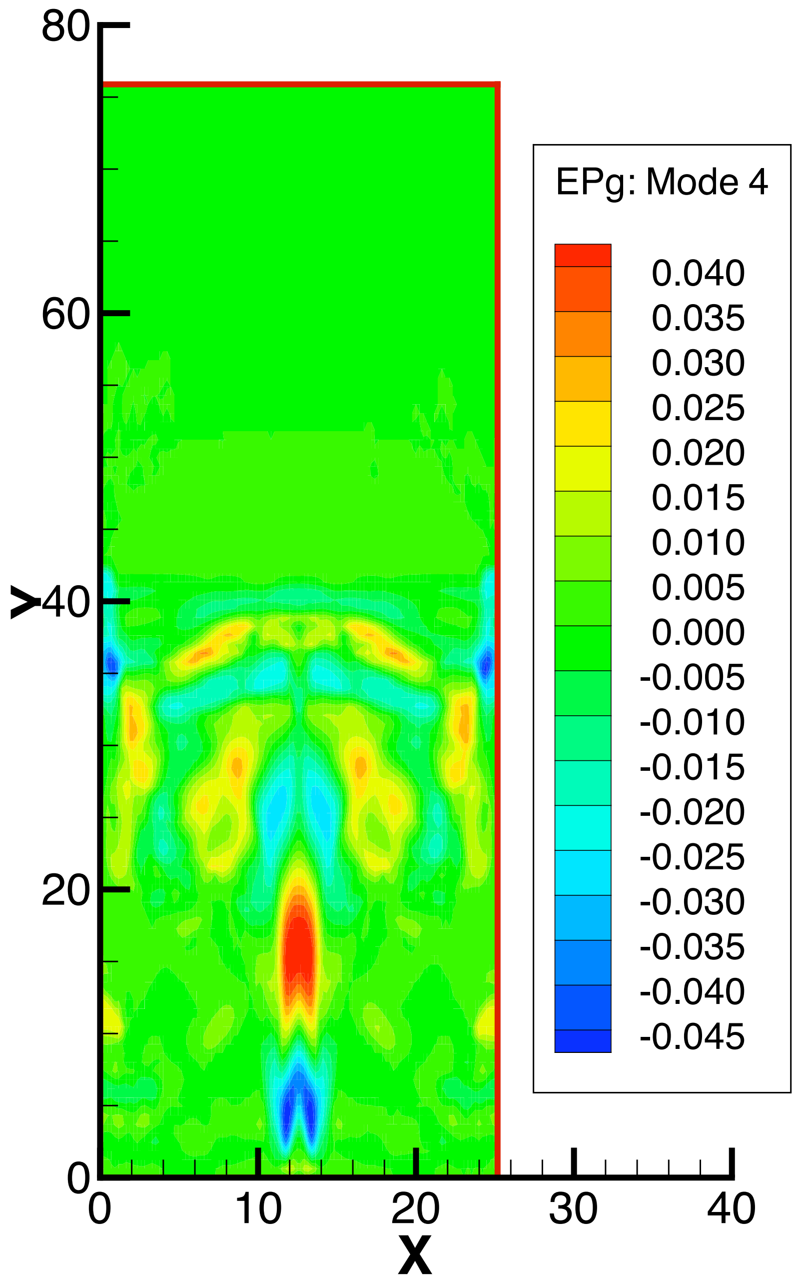

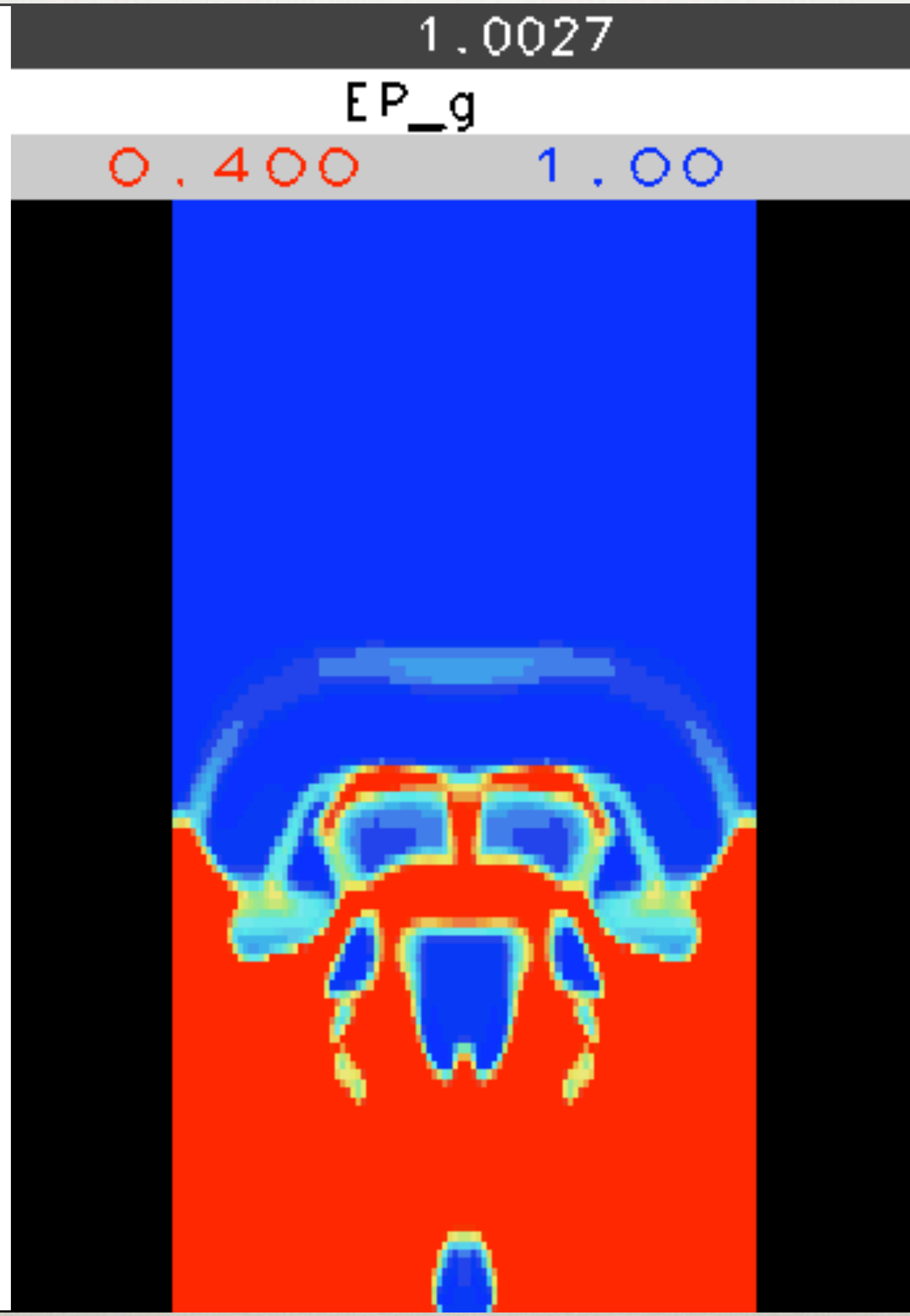

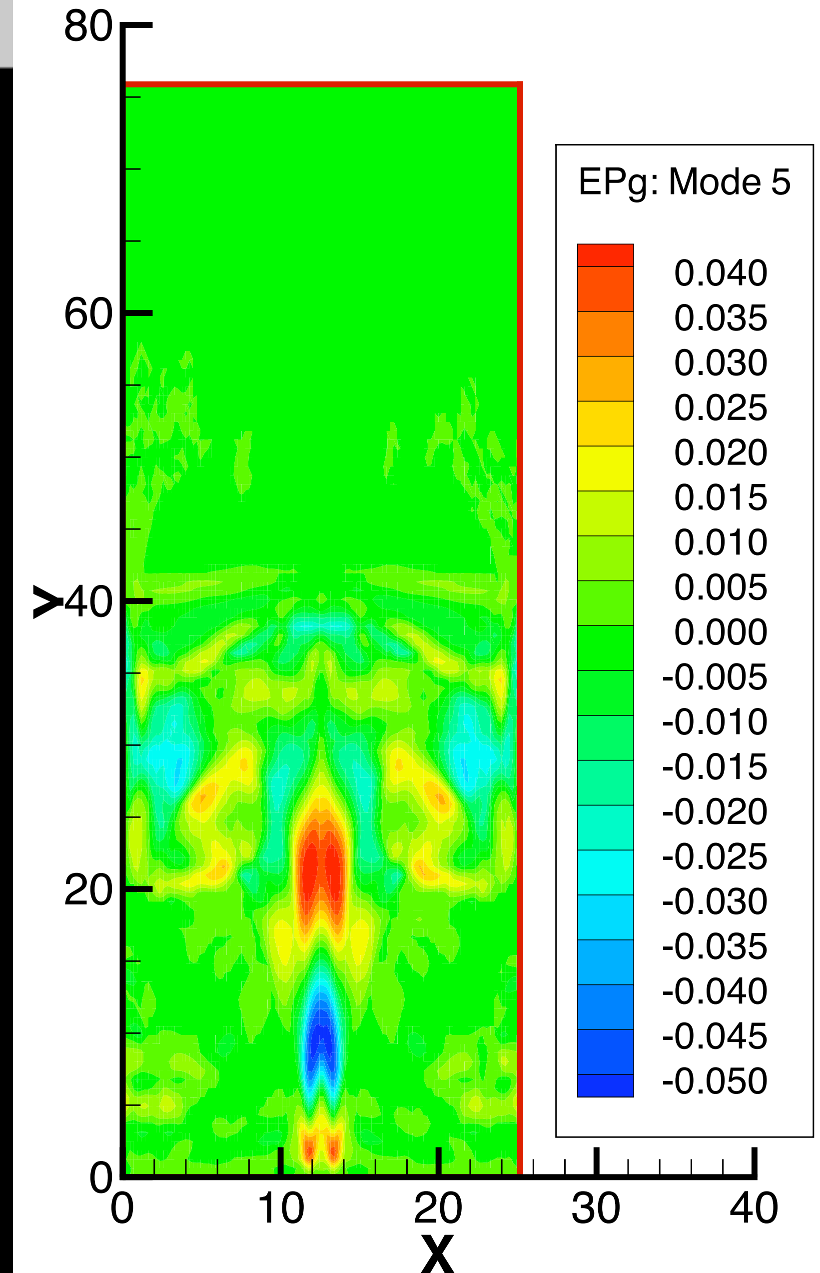

4th & 5th Time Coefficients & Fourier Transformation

4th

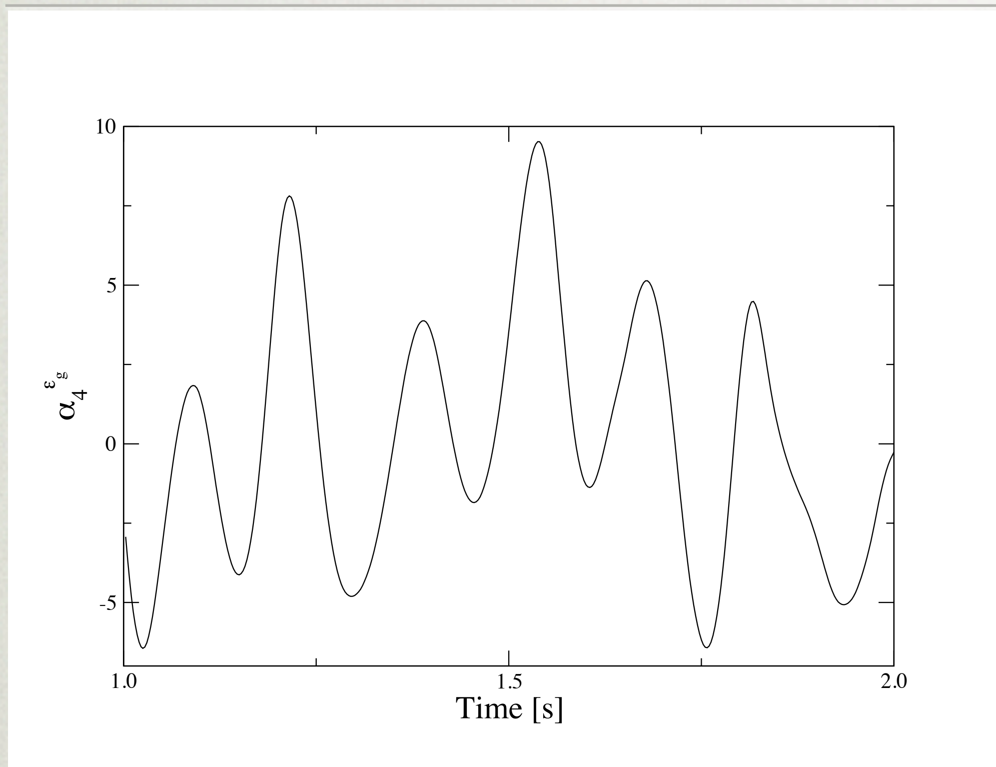

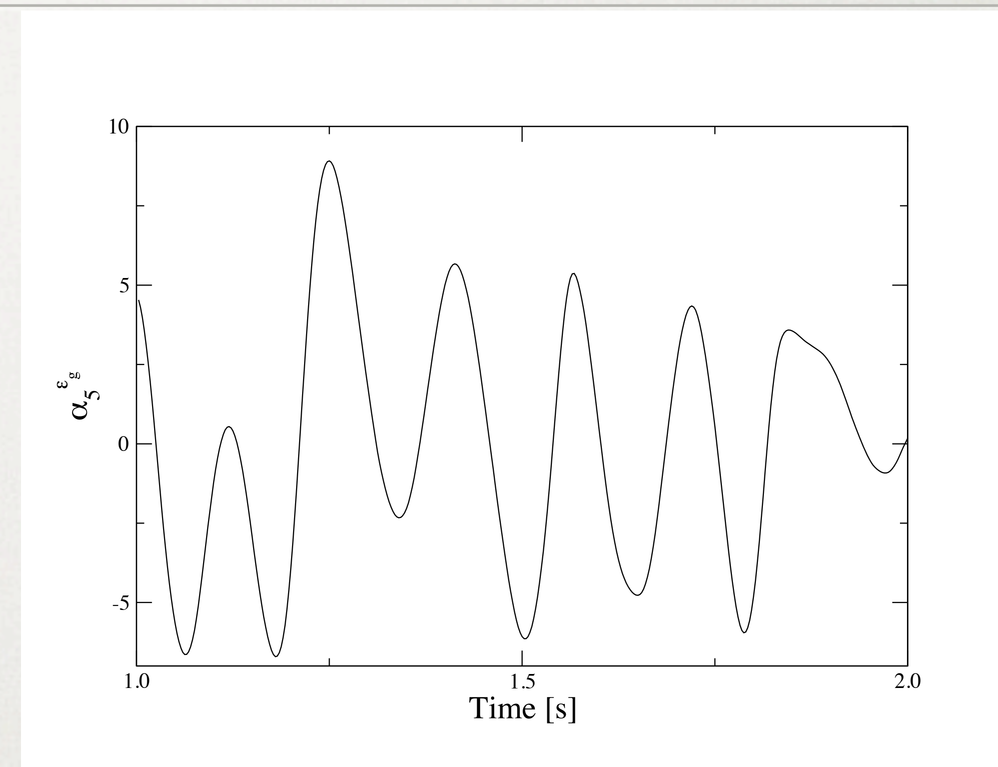

5th

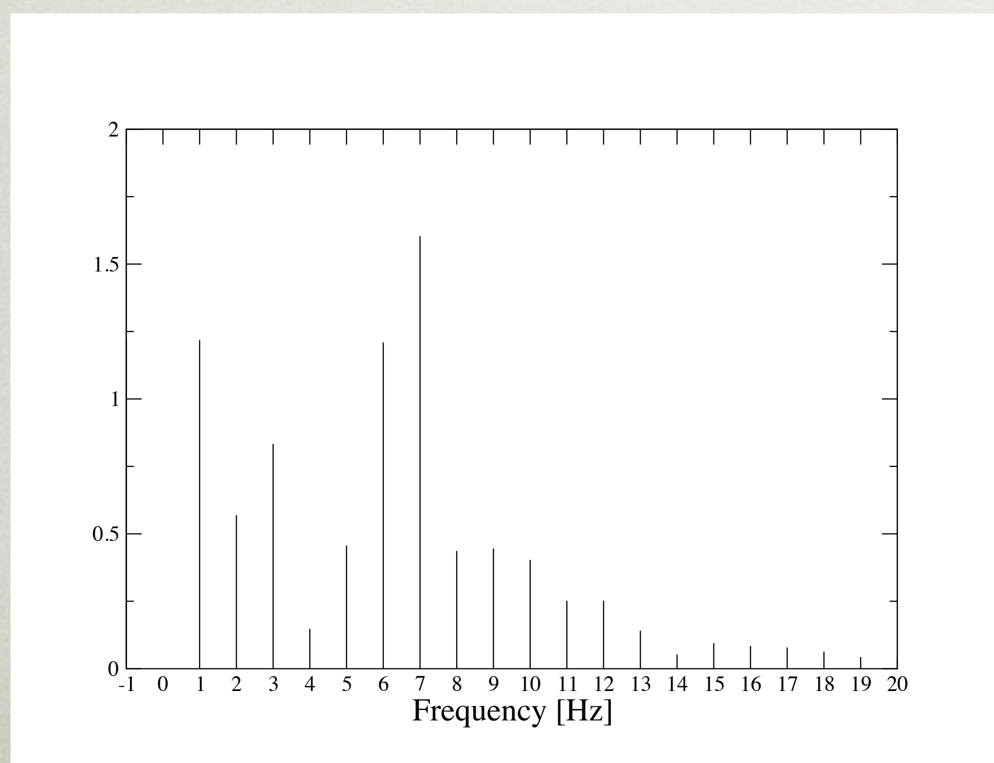

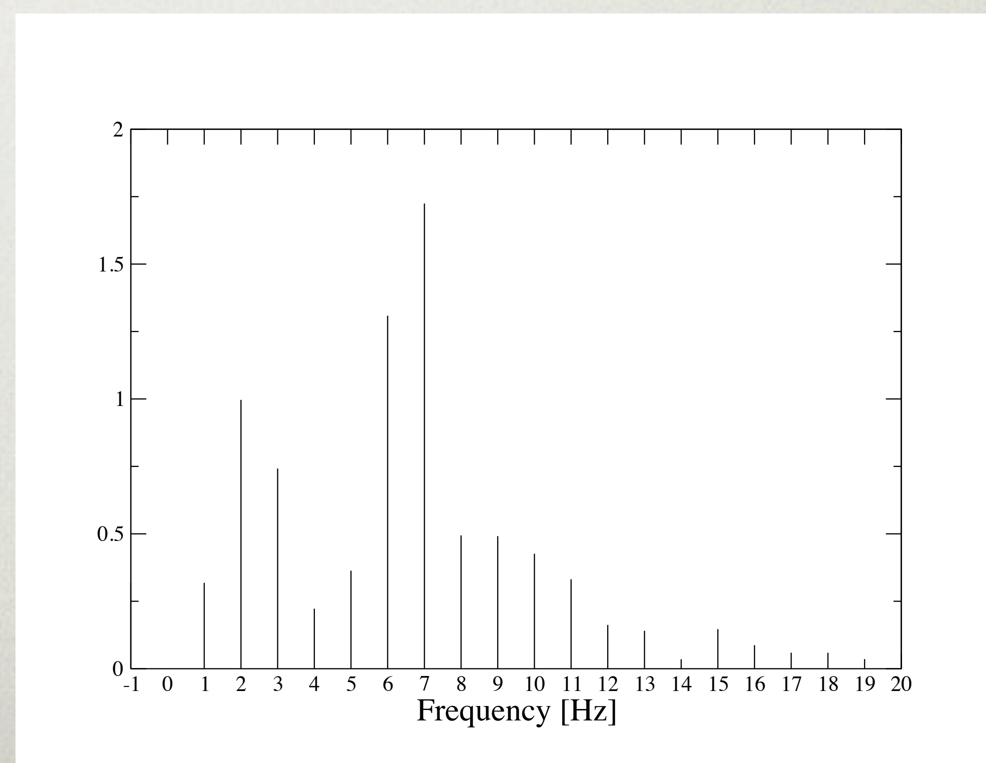

Void Fraction Reconstruction, t=1.5 sec.

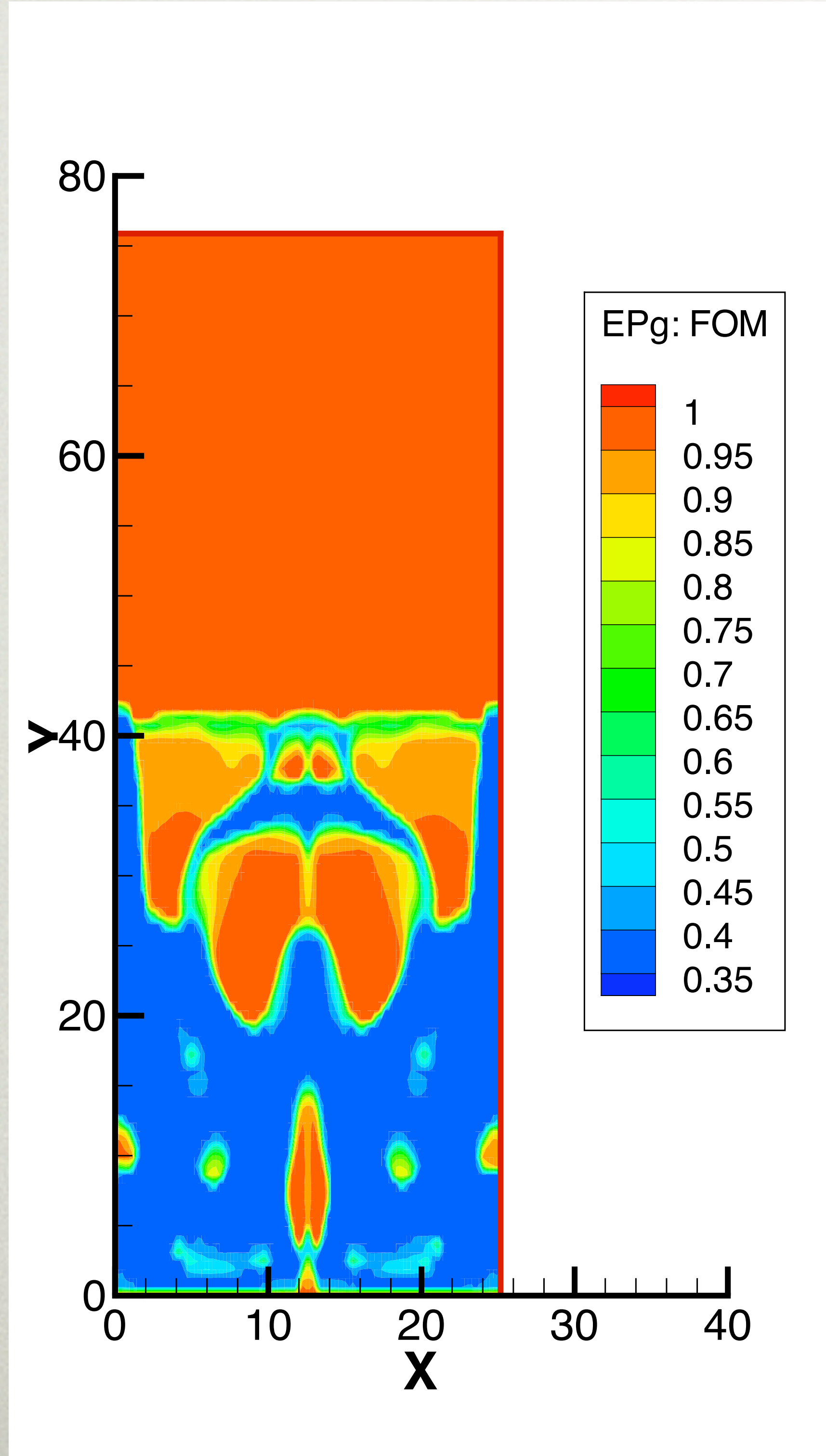

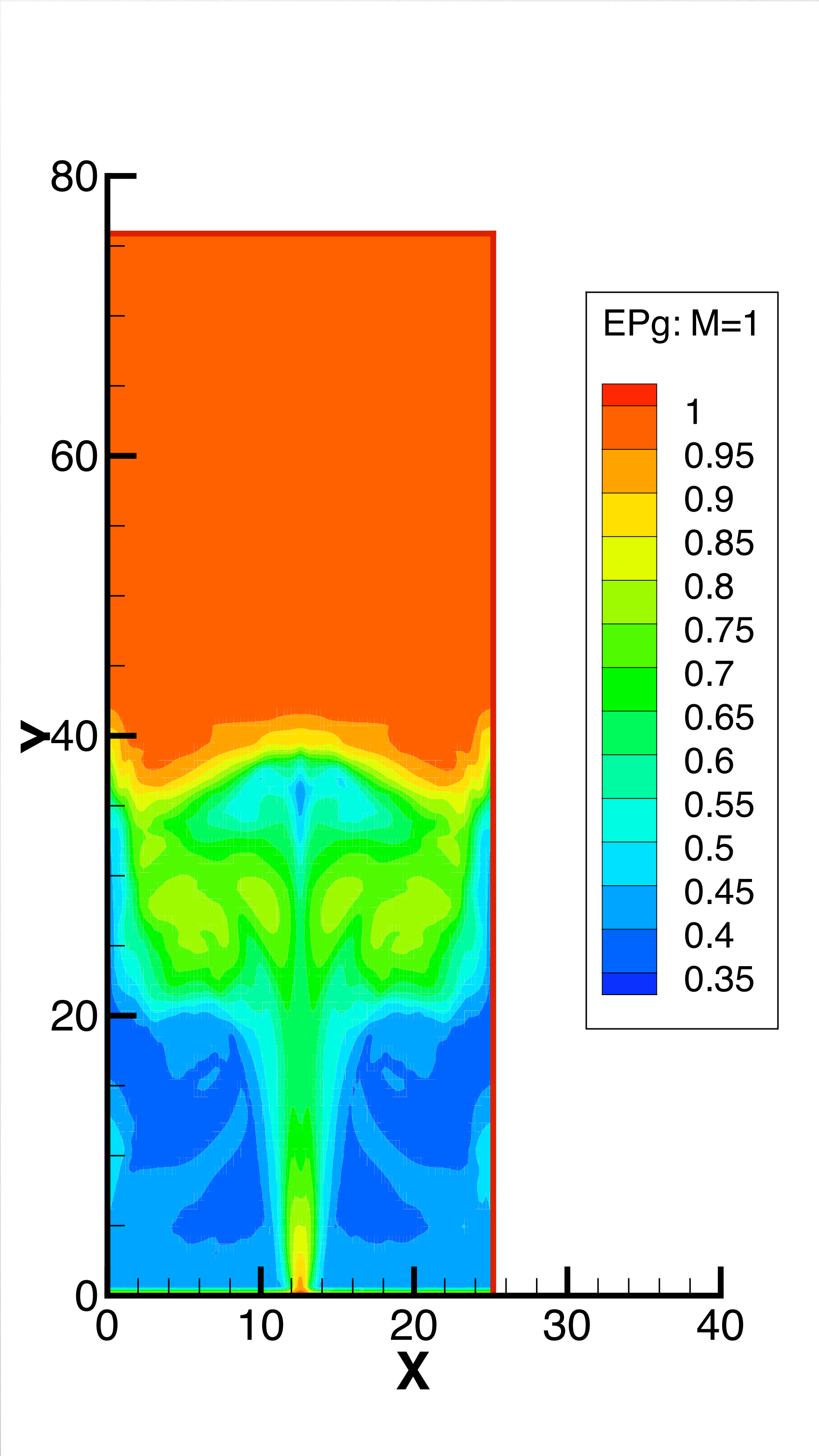

Moving Discontinuities & POD Bubbling Case

- Observations
  - some modes seem to be defining the bubble at a certain instant
  - reconstruction could produce unphysical results unless an excessive number of modes is used
- Needs
  - Augment POD by "bubble modes"
  - Track bubble location

Mathematical Morphology‡

- Theory and technique for analysis of spatial structures
- Based on set theory, integral geometry, and lattice algebra
- Developed to identify geometry of porous media
- Currently widely used in image analysis

‡ A. Haas, G. Matheron & J. Serra, "Morphologie mathematique et granulometries en place," *Annales des Mines,* XI pp. 736-53, XII pp 767-82, 1967

Operations

- Morphological
  - Erosion
  - Dilation
- Non-morphological
  - Blurring
  - Blur/erosion
  - Dilation/blur
  - Thresholding

Morphological Operations

- All operations performed on structuring elements (SE)
  - Used to probe image with desired shape
  - Assumes values of image
  - Elements oriented at 0, 45 ,90, and 135 degrees from horizontal
- All morphological operations based on two operators:
  - Erosion: (minimum shift in data on SE's)

$$erosion(f(i,j)) = \min(f(i+k, j+l) - b(k,l))$$

  - Dilation: (maximum shift in data on SE's)

$$dilation(f(i,j)) = \max(f(i-k, j-l) + b(k,l))$$

Non-Morphological Operations

- Blurring
  - Noise reduction technique
  - Operates on 3 point stencil
  - Defined as:

$$blur(i) = \frac{\sum_{p=i-L}^{i+L} f(p)}{K} \qquad L = \frac{K-1}{2}$$

- Pseudo-morphological operators:
  - blur/erosion

$$be(f) = blur(f) - erosion(blur(f))$$

  - dilation/blur

$$db(f) = dilation(blur(f)) - blur(f)$$

  - Applied after image is blurred and eroded/dilated
  - Used to eliminate obvious non-edges

Non-Morphological Operations

- Edge indicator:
  - Minimum of maximums of be and db operators
  - Will highlight all edges

$$Indicator(f) = \min(\max(db_i(f)), \max(be_i(f))) \qquad i = 1, \ldots, 4$$

- Thresholding
  - Image segmentation technique
  - Used to isolate areas of interest
  - Applied globally (binary fix) or semi-globally (0 outliers only)
  - Must be applied to gray-scale images
  - Example:

$$thres(Ind(f(i,j))) = 1 \quad \text{if} \quad \alpha \geq Ind(f(i,j)) \geq \beta$$

$$thres(Ind(f(i,j))) = 0 \quad \text{otherwise}$$

Bubble Detection

- t = 1s for V_{jet} = 355 cm/s
- Threshold applied for values α = .1 and β = .2
- Gives good edge representation (2 pt. ramp)

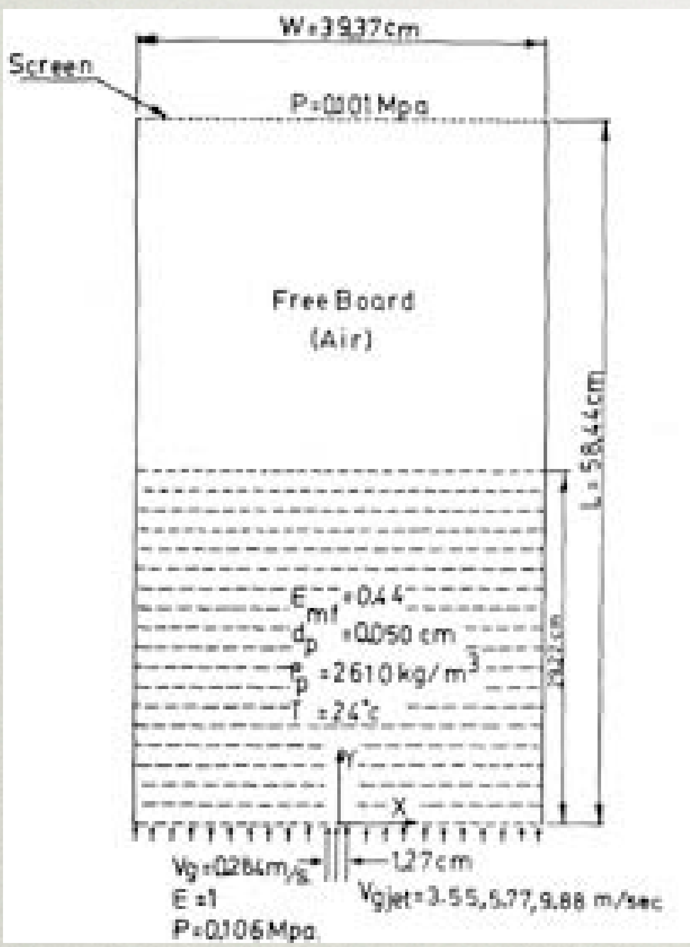

Bubbling Test Cases from *Multiphase Flow and Fluidization*, Gidaspow, p. 156.

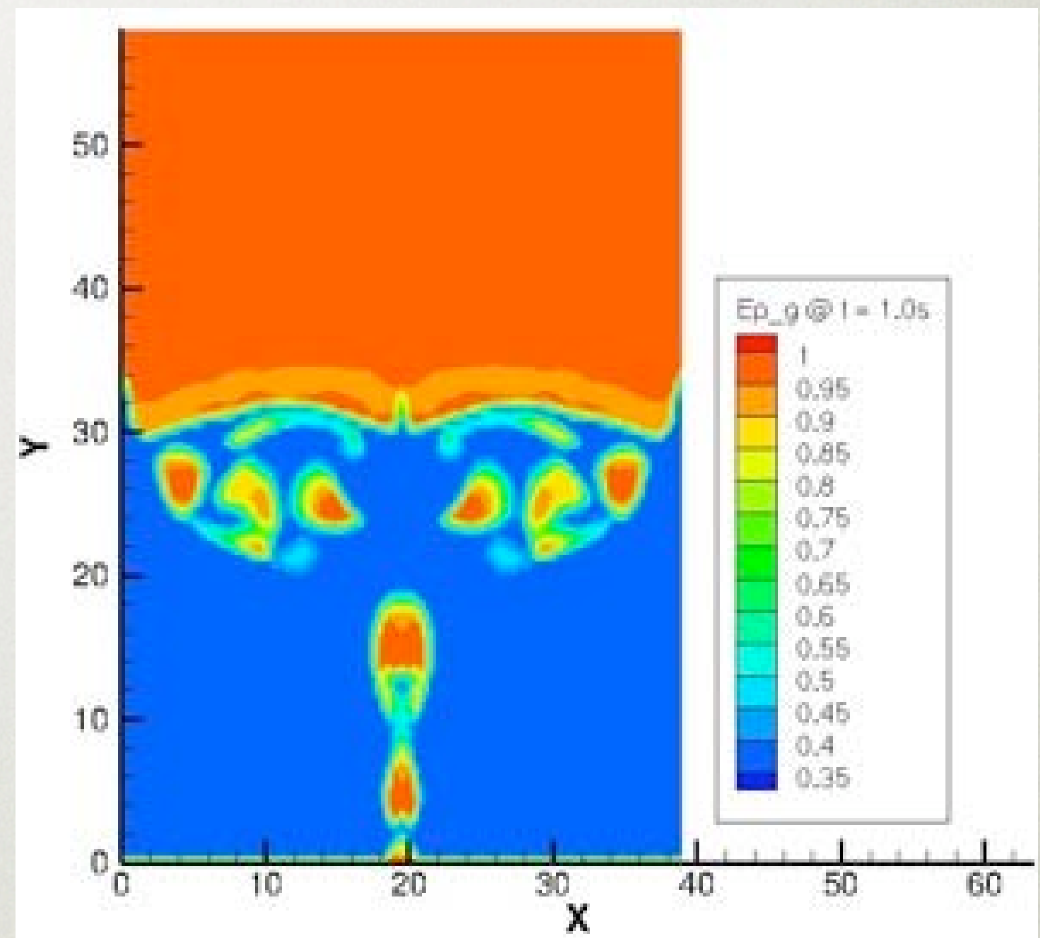

Void Fraction from MFIX @ t = 1.0 s.

Bubble Detection

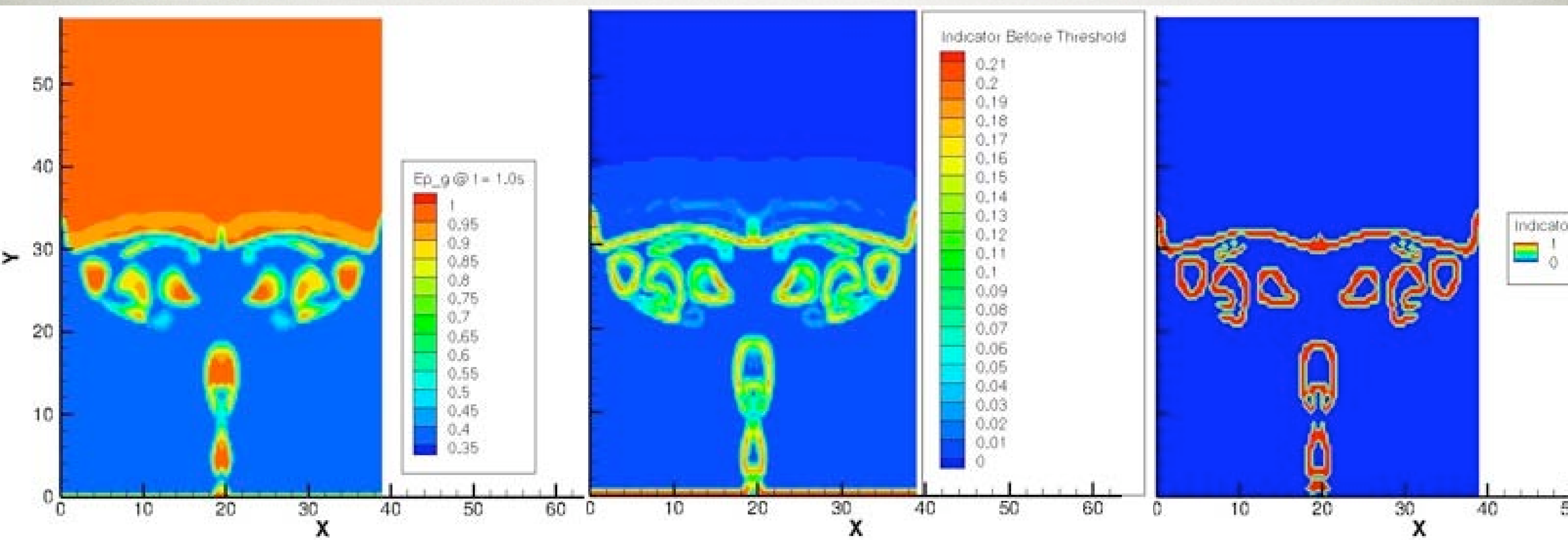

Void Fraction from MFIX @ t = 1.0 s.

Edge indicator before thresholding

Edge indicator after thresholding

Augmented POD

- Add "discontinuity modes" to set of POD basis functions
- Discontinuity modes could move and deform in time
- Hope:
  - Removes Gibbs phenomenon by capturing the discontinuity exactly

1D Test Case

- First-order wave equation used to simulate simple moving discontinuity

$$\frac{\partial u}{\partial t} + c\frac{\partial u}{\partial x} = 0$$

- Discretized as

$$u_i^{n+1} = u_i^n - \frac{c\Delta t}{\Delta x}(u_i^n - u_{i-1}^n)$$

1D Test Case (cont.)

- Simple quadratic solution is assumed

$$u(x,t) = a + b(x - ct) + d(x - ct)^2$$

- Discontinuity added at t=0 s according to

$$u(x,t=0) = \begin{cases} a + bx + dx^2 + 1 & x \le x_{s,0} \\ a + bx + dx^2 & x > x_{s,0} \end{cases}$$

Augmented POD for Wave Eq.

- Assume a POD approximation with a discontinuity mode

$$u(\mathbf{x}, t_k) = \phi_0(\mathbf{x}) + \sum_{j=1}^{m-1} \phi_j(\mathbf{x})\alpha_j(t_k) + \psi(\mathbf{x}, t_k)\beta(t_k)$$

- Use notation

$$\psi(\mathbf{x}, t_k) = \phi_m(\mathbf{x}, t_k), \qquad \beta(t_k) = \alpha_m(t_k), \qquad \alpha_0(t_k) \equiv 1$$

- Substitute in PDE

$$\frac{\partial}{\partial t}(\sum_{j=0}^{m} \phi_j(\mathbf{x}, t_k)\alpha_j(t_k)) + c\frac{\partial}{\partial x}(\sum_{j=0}^{m} \phi_j(\mathbf{x}, t_k)\alpha_j(t_k)) = 0$$

POD-ROM for Wave Eq. (cont.)

- A Galerkin projection onto the basis functions gives the system of equations

$$A\dot{\alpha} + B\alpha + d = 0$$

- where

$$[A]_{ij} = (\phi_j, \phi_i)$$

$$[B]_{ij} = \begin{cases} (c\phi'_j, \phi_i) & j = 1, \ldots, m-1 \\ (c\phi'_m, \phi_i) + (\dot{\phi}_m, \phi_i) & j = m \end{cases}$$

$$\{d\}_i = (c\phi'_0, \phi_i)$$

- System solved with a Runge-Kutta routine

Wave Equation Results

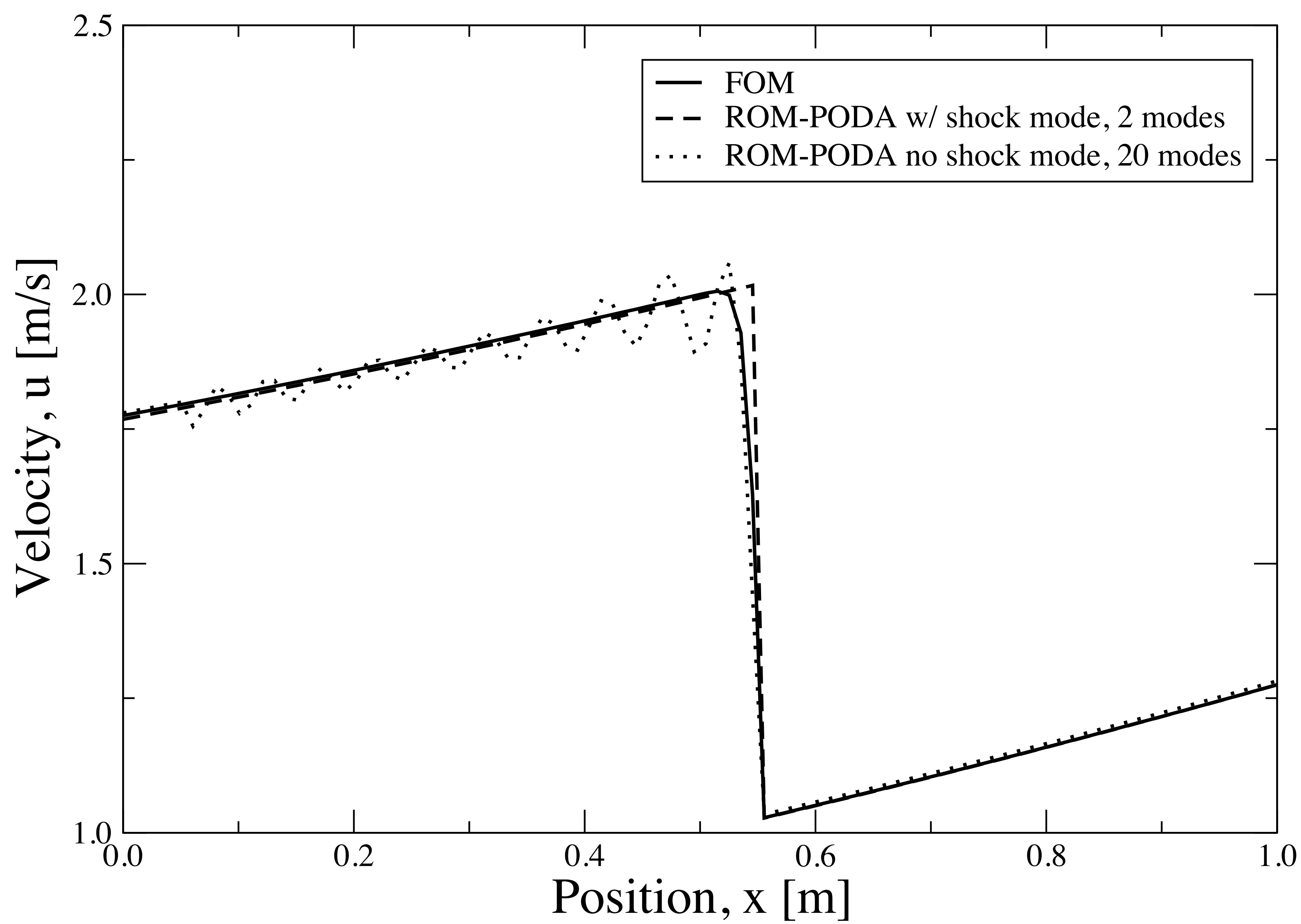

3D Implementation

POD Discretized (PODD) vs. POD Analytical (PODA)

PODD

- Substitute POD approximation into discretized governing equations
- Follows same solution algorithm as full-order model
- Easier to implement for void fraction and pressure correction algorithms

PODA

- Substitute POD approximation into governing PDEs
- Allows any spatial/temporal discretizations and integration strategies for resulting ODEs
- More difficult to implement for void fraction and pressure

3D Implementation of POD for MFIX

- Current approach uses PODD method, but PODA method should also be explored
- ODEx 3D (3D POD code) is being tested as a 2D code with third dimension k=1

Conclusions & Future Work

Conclusions

- 3D POD version of MFIX is on schedule and budget
- Morphology can capture bubble location and shape
- In a simple case, POD approximation augmented by a discontinuity mode to capture the moving discontinuity
- Optimal distribution of snapshots in time depends on time scale of problem

Future Work

- Finish 3D POD of MFIX
- Extend augmented POD
  - Burgers' equation
  - 2D flow
- Develop a method for predicting bubble location at next time instant
- Apply augmented POD to multiphase flow

Thank you!
Questions?